# General Disclaimer

## One or more of the Following Statements may affect this Document

- This document has been reproduced from the best copy furnished by the organizational source. It is being released in the interest of making available as much information as possible.

- This document may contain data, which exceeds the sheet parameters. It was furnished in this condition by the organizational source and is the best copy available.

- This document may contain tone-on-tone or color graphs, charts and/or pictures, which have been reproduced in black and white.

- This document is paginated as submitted by the original source.

- Portions of this document are not fully legible due to the historical nature of some of the material. However, it is the best reproduction available from the original submission.

PRECURSOR IONIZATION EFFECTS ON MAGNETOHYDRODYNAMIC

SWITCH-ON SHOCK STRUCTURE

by

Martin I. Hoffert

Department of Aeronautics and Astronautics

$$K'_{eq}(T') = 2.90 \times 10^{22} T'^{3/2} \exp\left(-\frac{\theta'_{ion}}{T'}\right) \ (m^{-3}) \tag{3}$$

where $\theta_{ion} = 1.831 \times 10^5 \ °K$ is the (first) "ionization temperature".

If $k'_{f_e}(T')$ is the production rate for electron-impact reactions, then from the principle of detailed balancing the corresponding three-body recombination rate is $k'_{r_e} = k'_{f_e}/K'_{eq}$. Thus, the electron production rate by Eq.(1a) may be written

$$(\dot{n}'_e)_e = k'_{f_e}(T')n'_e\left[n'_A - \frac{n'^2_e}{K'_{eq}(T')}\right]$$

Consistent with the single-temperature, ground-state ionization model assumed previously, we can use the expression for $k'_{f_e}$ given by the formula and (argon) data in Zel'dovich and Raizer[10].

$$k'_{f_e}(T') = 1.07 \times 10^{-21} T'^{3/2}\left(\frac{\theta'_{ion}}{T'} + 2\right) \exp\left(-\frac{\theta'_{ion}}{T'}\right) \ (m^3/sec) \tag{4}$$

As in Ref. 6, we let $Q'_{eA}$ and $Q'_{eI}$ be the elastic collision cross-sections for electron-atom and electron-ion collisions. The electrical conductivity can then be written[6] as

$$\sigma = \frac{e^2}{m_e}\left(\frac{\pi m_e}{8kT'}\right)^{\frac{1}{2}} \frac{n'_e}{(n'_A Q'_{eA} + n'_e Q'_{eI})} \tag{5}$$

where $m_e = 9.107 \times 10^{-31} kg$ is the mass of an electron, $e = 1.602 \times 10^{-9} C$ is the charge of an electron and $k = 1.380 \times 10^{-23} J/°K$ is Boltzmann's constant. Also, following Refs. 6 and 7, a reference degree of ionization is introduced,

NEW YORK UNIVERSITY
New York, New York

PRECURSOR IONIZATION EFFECTS ON MAGNETOHYDRODYNAMIC

SWITCH-ON SHOCK STRUCTURE

by

Martin I. Hoffert
Research Scientist
Department of Aeronautics and Astronautics

March 1969

## ABSTRACT

The influence of shock-induced precursor ionization on the steady-state structure of switch-on shock waves with nonequilibrium ionization and radiation is examined theoretically. A single-temperature monatomic gas is assumed, together with a Clarke-Ferrari model for photoionization of the upstream gas. It is found that the effect of the precursor depends in general on the ratio of a characteristic precursor length to a characteristic magnetic interaction length. For the slightly ionized case treated in some detail, this ratio is much greater than unity, indicating a precursor-independence for the magnetohydrodynamic shock structure.

# TABLE OF CONTENTS

# LIST OF FIGURES

## NOMENCLATURE

$B'; B$      = magnetic field intensity$(w/m^2)$; $B'/B_{x_1}$

$B'_{ion}$      = frequency-integral of Planck function$[J/(m -sec)]$, Eq.(8a)

$c$      = velocity of light $(2.998 \times 10^8 \text{ m/sec})$

$e$      = electron charge $(1.602 \times 10^{-9} \text{ C})$

$E'; E$      = electric field intensity (V/m); $E/(u'_{x_1} B'_{x_1})$

$f$      = dimensionless function; Eq.(22)

$g$      = dimensionless function; Eq.(21)

$h$      = Planck's constant $(6.625 \times 10^{-34} \text{ J-sec})$

$i'$      = static enthalpy $(J/°K)$

$k$      = Boltzmann's constant $(1.380 \times 10^{-23} \text{ J/°K})$

$k_1$      = constant defined by Eq.(31)

$k'_{f_e}; k_{f_e}$      = forward ionization rate parameter for electron-atom impacts $(m^3/\text{sec})$; $k'_{f_e}/[(2)^{\frac{1}{2}} Q'_{AA_1} u'_{x_1}]$

$k'_{r_e}$      = three-body recombination rate for electron-impact reactions $(m^6/\text{sec})$

$K'_{eq}; K_{eq}$      = equilibrium constant $(1/m^3)$; $K'_{eq} m_A/\rho'_1$

$\ell_1$      = $\lambda'_1/\lambda'_r$ , a constant

$m_A$      = atomic mass (kg)

$m_e$      = electron mass $(9.107 \times 10^{-31} \text{ kg})$

$M$      = Mach number

$M_A$      = Alfven number

$n'$      = global number density $(1/m^3)$

$n'_A$      = atom number density $(1/m^3)$

$n'_e$      = electron number density $(1/m^3)$

$(\dot{n}'_e)_e$      = electron production rate due to electron-impact reactions $[1/(m^3-sec)]$

$(\dot{n}'_e)_r$      = electron production rate by photoionization $[1/(m^3-sec)]$

$p'$ = static pressure $(N/m^2)$

$q_r';q_r$ = radiative heat flux $[J/(m^2\text{-sec})]$; $q_r'/(\rho_1'u_{x_1}'R\Theta_{ion}')$

$Q_{AA}'$ = atom-atom elastic collison cross-section $(m^2)$

$Q_{eA}'$ = electron-atom elastic collision cross-section $(m^2)$

$Q_e'$ = electron-ion (Coulomb) collision cross-section $(m^2)$

$Q_r'$ = photoionization cross-section at ionization edge $(m^2)$

$R$ = $k/m_a$ = gas constant $[J/(kg - {}^\circ K)]$

$R_m$ = $\sigma'\mu_o u_{x_1}\lambda_1'$ = magnetic Reynolds number

$S';S$ = source function $[J/(m^2\text{-sec})]$; $S'/(\rho_1'u_{x_1}'R\Theta_{ion}')$

$T';T$ = gas temperature $({}^\circ K)$; $T'/T_1'$

$u';u$ = gas velocity in shock-frame (m/sec); $u'/u_{x_1}'$

$x';x$ = streamwise coordinate (m); $x'/\lambda_1'$

$\ddot{x}$ = transformed x-coordinate, Eq.(32)

$y'$ = transverse (radial) coordinate (m)

$z'$ = transverse (azimuthal) coordinate (m)

$\alpha$ = degree-of-ionization

$\alpha_{eq}$ = reference (equilibrium) degree-of-ionization

$(\dot{\alpha}')_e$ = degree-of-ionization production rate by electron impacts (1/sec)

$(\dot{\alpha}')_r$ = degree-of-ionization production rate by photoionization (1/sec)

$\epsilon_1,\epsilon_2$ = constants defined by Eqs.(23a,b)

$\Theta_{ion}',\Theta_{ion}$ = ionization "temperature" $({}^\circ K)$; $\Theta_{ion}'/T_1'$

$\lambda'$ = atom-atom mean free path (m)

$\lambda_r'$ = photon-atom mean free path at ionization edge (m)

$\mu_o$ = magnetic permeability in vacuo $(4\pi \times 10^{-7} N/A^2)$

$\nu'$      = photon frequency (1/sec)

$\rho'; \rho$      = gas density ($kg/m^3$); $\rho'/\rho_1'$

$\sigma'$      = electrical conductivity [1/(ohm - m)]

subscripts

1      = upstream of shock

2      = downstream of shock

A      = atom specie

e      = electron specie

I      = ion specie

ion      = ionization energy

s      = imbedded shock location

x      = $x'$-direction

y      = $y'$-direction

z      = $z'$-direction

# 1. Introduction

The use of annular electromagnetic shock tubes to produce laboratory scale plasmas has motivated a number of theoretical studies of "switch-on" hydromagnetic shock waves, thought to propagate in these devices[1-7].

When the gas is initially ionized and electrically conducting, the transition from the upstream to the downstream state is a pure magnetohydrodynamic shock wave whose structure (for a perfect gas) was treated theoretically by Bleviss[1]. If, on the other hand, the upstream gas is electrically non-conducting, the magnetrohydrodynamic jump conditions are no longer mathematically sufficient to relate upstream and downstream states. This latter type is commonly termed a gas-ionizing hydromagnetic shock and has been discussed by Gross[2], Taussig[3,4], Perona and Axford[5] and others. It was shown in these works that the condition of zero upstream electrical conductivity leads to an indeterminacy in the value of the electric field in front of the shock. Recourse must then be made to other physical principles to define the jump conditions, i.e. a magnetohydrodynamic analogy of the Chapman-Jouget hypothesis[2]. These considerations, in turn, relate to the present interest in the effect of precursor ionization on switch-on shocks. In view of the electrical conductivity requirement, not only the details of structure, but the very existence of the more general gas-ionizing switch-on shocks, can be influenced by precursor effects. In the present study we are primarily concerned with the effect of precursor ionization, caused by photoionization of the cold upstream gas by the hot downstream portion of the shock, on the overall structure of "switch-on" shocks.

The significance of precursor ionization has been discussed previously[6] in the context of the more general hydromagnetically oblique shock fronts encompassing both fast and slow shocks. It was shown there that if a gasdynamic shock was required to "trigger" the ionizing reactions leading to electrical conductivity in the gas, then (for the monatomic gas model used in that work) only slow solutions could be constructed.

On the other hand, it was recognized that gas in front of the shock could be made electrically conducting by a radiation-induced precursor mechanism, thus providing a physical basis for fast shock structures. Since the switch-on shock (the subject of interest in the shock tube case) is magnetohydrodynamically fast the effect of such precursors has considerable practical interest.
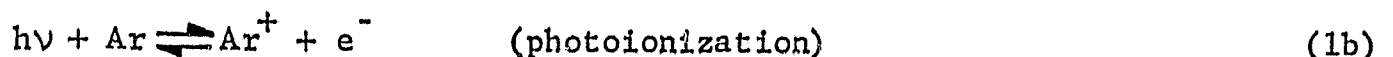
Figure 1a illustrates the geometry of an annular electromagnetic shock tube and the way in which a steady-state shock front can be generated in the annular space. Under appropriate conditions of density, magnetic and electric field strength, etc., the switch-on mode of operation is anticipated: when the axial magnetic field $B'_{x_1}$ is applied through the solenoid coils and an electric field $E'_{y_1}$ is simultaneously applied radially across the channel, an ionized shock front is driven into the quiescent gas with velocity $u'_{x_1}$. We denote the upstream and downstream states of the shock by subscripts 1 and 2 respectively, in shock fixed coordinates. The transverse components of velocity and magnetic field are initially zero ($u'_{z_1} = B'_{z_1} = 0$) as depicted in Fig. 1b ; however, within the shock front structure, these transverse components are induced or switched on so that $u'_{z_2} \neq 0$; $B'_{z_2} \neq 0$.

2

In what follows, the switch-on shock is analysed in conjunction with a simple precursor model due to Clarke and Ferrari in order to determine the effect on the overall structure. The actual physical situation involves coupled phenomena of radiation, chemical nonequilibrium and magnetohydrodynamic interaction; and these effects are all included in the model. However, to make the relations more explicit the analysis is carried out for a monatomic, singly ionizing, single-temperature gas. Numerical constants are evaluated for argon but generalization of this analysis to other monatomic gases is straightforward. If monatonic hydrogen is chosen the analysis has astrophysical interest.

Expressions governing the radiative heat flux, the photoionization rate and electron-atom impact ionization rates are developed in Section 2. These relations together with the one-dimensional conservation and Maxwell equations described in Section 3 are the governing equations for overall shock structure. In Section 4 certain important properties of the integral curves of this system are discussed, in particular, the question of whether the shock is fully or only partly dispersed by magnetic induction effects. In Section 5, the shock structure is analyzed for the special case of a slightly ionized gas. Finally, conclusions are drawn in Section 6 regarding the significance of precursor effects in general.

## 2. Radiative Heat Flux and Ionization Rates

Prior to analysis of the shock front per se, a radiation and ioni - zation model applicable within the shock structure will be developed. It will be assumed that the only reactions of any significance in electron-production have the form,

3

$$e^- + Ar \rightleftharpoons Ar^+ + e^- + e^- \quad \text{(electron-impact)} \tag{1a}$$

$$h\nu + Ar \rightleftharpoons Ar^+ + e^- \quad \text{(photoionization)} \tag{1b}$$
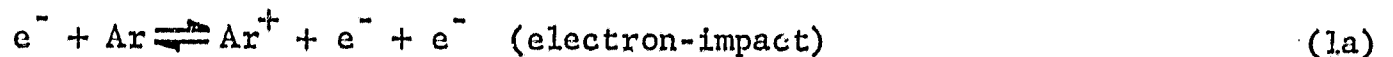
These are the same set of reactions studied by Clarke and Ferrari[8] in their treatment of simultaneous chemical and radiative nonequilibrium in shock waves. Moreover, it is assumed that atoms are in their ground state so that ionization will only take place when the collision with a photon ($h\nu$) or an electron ($e^-$) impact can provide more energy than the first ionization potential. Recently, an alternate non-thermal absorption process has been proposed by Vulliet[9]: photons emitted by the hot post-shock-gas from the resonance line near the wings are first absorbed by upstream atoms; these excited atoms then absorb and thermalize the far wing and continuum by photoionization. This results in resonance radiation heating of the preshocked gas. A steady state is reached when the moving shock engulfs energy at the same rate it radiates it. Therefore, one expects a larger electron concentration farther ahead of the shock than given by the Clarke-Ferrari model used here, since only the energy in the continuum above the ground state ionization energy is absorbed and thermalized. Nevertheless, from the point of view of shock structure, the major conclusions based on the present simplied model are expected to remain valid, even if a more complex resonance radiation model or multi-temperature model were employed as will be discussed subsequently.

We now turn to the derivation of nonequilibrium equations for ionization and radiation. Henceforth; "primes" are used to denote physical (dimensional) quantities as distinguished from dimensionless

"unprimed" quantities, to be introduced shortly. Rather than deal directly with electron, atom and global number densities, $n_e$, $n_A$ and $n'(= n_A + 2n_e)$ we work directly with the degree-of-ionization $\alpha$ since this single quantity together with the gas density $\rho'$ specifies the number densities. Let,

$$\alpha \equiv \frac{n_e'}{n_e' + n_A'} \quad ,$$

with the properties

$$n_e' = \frac{\alpha \rho'}{m_A} \quad , \qquad n_A' = \frac{(1 - \alpha)\rho'}{m_A} \quad , \quad n' = \frac{(1 + \alpha)\rho'}{m_A} \tag{2}$$

where $m_A = 6.628 \times 10^{-26}$ kg is the mass of an atom and $\rho'$ is the mass density of the mixture. In a separate analysis, it was shown that the influence of a distinct electron temperature $T_e' \neq T'$ on the Clarke-Ferrari precursor model would be to decrease the predicted length of the precursor. Since the Clarke-Ferrari single-temperature model is known to underestimate experimentally observed precursor lengths, there is. little to be gained by considering a more complex two-temperature model in the context of the present analysis. The qualitative of effect of more realistic precursor models is significant however and is treated in Section 6. For the overall reaction path $Ar \rightleftharpoons Ar^+ + e$, an equilibrium "constant",

$$K_{eq}' (T') \equiv \left( \frac{n_e'^2}{n_A''} \right)_{eq}$$

which depends only on temperature $T'$ is derivable from statistical mechanics. For argon[7], this takes the form

$$\alpha_{eq}(T',\rho',\alpha') \equiv \left[1 + \frac{\rho'(1 + \alpha)}{m_A K'_{eq}(T')}\right]^{-\frac{1}{2}} \quad , \tag{6}$$

which corresponds to local thermodynamic equilibrium at number density $n'$ and temperature $T$. It is to be distinguished from the "$\alpha_E$" used by Clarke and Ferrari[8] but is related to the latter by the equation

$$\frac{\alpha_E^2}{1 - \alpha_E} = \frac{(1 + \alpha)\alpha_{eq}^2}{1 - \alpha_{eq}^2}$$

The bound-free continuum photoionization model used here is, with minor modifications, the same as that described in Ref. 8. In comparing the two, the foregoing relation should be borne in mind. Making use of Eqs.(2) and (6) the degree-of-ionization production rate by electron-impacts is

$$\dot{\alpha}'_e \equiv \frac{m_A (\dot{n}'_e)_e}{\rho'} = k'_{f_e}(T') \left(\frac{\rho'}{m_A}\right) \left(\frac{\alpha}{1 + \alpha}\right) \left[1 - \left(\frac{\alpha}{\alpha_{eq}}\right)^2\right] \tag{7}$$

The other ionizing process is photoionization which occurs when the incident photon has a frequency $\nu'$ equal to or greater than the "ionization edge" frequency $\nu'_{ion} = k\Theta_{ion}/h = 3.81 \times 10^{15} \text{sec}^{-1}$, where $h = 6.625 \times 10^{-34}$ J-sec is Planck's constant. For temperatures of interest have $kT' \ll h\nu'_{ion}$ so we can write the Planck function

$$B'_\nu(T') \equiv \frac{2h\nu'^3}{c^2\left[\exp(h\nu'/kT')-1\right]} \approx \frac{2h\nu'^3}{c^2} \exp\left(-\frac{h\nu'}{kT'}\right) \quad ,$$

where $c = 2.998 \times 10^8$ m/sec is the velocity of light in vacuo. Since the radiant energy active in bound-free photoionization is above the ionization

edge, the frequency integral,

$$B'_{ion}(T') \equiv \int_{\nu'_{ion}}^{\infty} B'_{\nu}(T')d\nu' \approx \frac{2\nu'^3_{ion}kT'}{c^2} \exp\left(- \frac{\Theta'_{ion}}{T'}\right)$$

(8a)

$$\approx 1.7 \times 10^7 \cdot T' \exp\left(- \frac{\theta'_{ion}}{T'}\right) \left(\frac{J/m^2}{sec}\right)$$

appears in the theory. Also, in the presence of simultaneous chemical and radiative non-equilibrium, Clarke and Ferrari showed that the appropriate grey-gas source function is

$$S'(T',\rho',\alpha) \equiv \frac{\alpha^2(1 - \alpha^2_{eq})}{\alpha^2_{eq}(1 - \alpha^2)} B'_{ion}(T')$$

(8b)

A similar source function can be obtained for a two-temperature gas, where the electrons may be either hotter or cooler than the background of atoms and ions, $Te' \neq T'$. The form is formally identical to Eq.(8b) with $T'_e$ as an argument rather than $T'$.

The relevant physical dimensions for photoionization by Eq.(1b) turns out to be the photon mean free path

$$\lambda'_r \equiv \frac{m_A}{\rho'(1 - \alpha)Q'_r}$$

(9)

based on the photo-cross-section at the ionization edge. The experiments of Rustgi[11] and other sources give this as $Q'_r = 3.6 \times 10^{-21} m^2$.

If the integro-exponential function of order two defined by $E_2(z) = \int_0^1 \exp\left(-\frac{z}{t}\right) dt$ is approximated by $E_2(z) \approx \exp\left[-(3)^{\frac{1}{2}}z\right]$, as suggested for example by Vincenti and Kruger[11] then a <u>differential equation</u> is obtainable from Ref. 8 for the radiative heat flux above the ionization edge $q_r'$, which takes the form,

$$\lambda_r' \frac{d}{dx'}\left(\lambda_r' \frac{dq_r'}{dx'}\right) = 3q_r' + 4\pi\lambda_r' \frac{dS'}{dx'} \tag{10}$$

Moreover, the Clarke-Ferrari theory shows that the electron production rate per unit volume by photoionization is related to the gradient of $q_r'$ through

$$(\dot{n}_e')_r = -\frac{1}{k\Theta_{ion}'} \cdot \frac{dq_r'}{dx'}$$

Defining a degree-of-ionization production rate as we did in Eq. (7) gives

$$\dot{\alpha}_r' \equiv \frac{m_A(\dot{n}_e')_r}{\rho'} = -\frac{1}{\rho'R\Theta_{ion}'} \cdot \frac{dq_r'}{dx'} \tag{11}$$

Neglecting diffusion, the conservation of electron (or ion) mass equation in one dimensional geometries is simply $u'(d\alpha/dx') = \dot{\alpha}_e' + \dot{\alpha}_r'$ or using Eq. (7)

$$u' \frac{d\alpha}{dx'} = k_{f_e}'(T')\left(\frac{\rho'}{m_A}\right)\left(\frac{\alpha}{1-\alpha}\right)\left[1 - \left(\frac{\alpha}{\alpha_{eq}}\right)^2\right] + \dot{\alpha}_r' \tag{12}$$

3. <u>Governing Dimensionless Equations</u>

We choose as the characteristic length for the overall shock structure problem the mean free path of the undisturbed gas upstream of the shock

9

$$\lambda_1' = \frac{m_A}{\rho_1'(1-\alpha)Q_{AA_1}'} \quad ,$$

where $Q_{AA_1}$ is the atom-atom elastic collision cross-section in the undisturbed gas. If $T_1' = 300°K$, $Q_{AA_1}' = 4 \times 10^{-19}m^2$.

Referring now to Fig.(1b) the following dimensionless (unprimed) variables and functions are defined in terms of upstream (state 1) values:

$$x = x'/\lambda_1' \; , \rho = \rho'/\rho_1', \; T = T'/T_1' \; , \; \Theta_{ion} \equiv \Theta_{ion}'/T_1' \; ,$$

$$\vec{u} = \vec{u}'/u_{x}' \quad , \; \vec{B} \equiv \vec{B}'/B_{x_1}' \; , \; \vec{E} \equiv \vec{E}'/(u_{x_1}' B_{x_1}') \; , \; \vec{q}_r - \vec{q}_r'/(\rho_1' u_{x}' R\Theta_{ion}')$$

$$\text{(14)}$$

$$R_m \equiv \sigma\mu_0 u_{x_1}' \lambda_1' \; , \; k_{f_e} \equiv k_{f_e}' \rho_1' \lambda_1'/(m_A u_{x_1}') \; , \; S \equiv S'/(\rho_1' u_{x}' R\Theta_{ion}')$$

$$K_{eq} \equiv K_{eq}' m_A/\rho_1' \; , \; F \equiv \left[Q_{eA}' + \alpha(Q_{eI}' - Q_{eA}')\right] / Q_{AA}'$$

where $\mu_0 = 4\pi \times 10^{-7}N/A^2$ is the magnetic permeability in vacuo. In the above $\vec{u}$, $\vec{B}$, $\vec{E}$ and $\vec{q}_r$ are the dimensionless velocity, magentic field, electric field and radiative heat flux vectors; Rm, $k_{f_e}$, S and $K_{eq}$ are the dimensionless magnetic Reynolds number, electron-impact rate, source function and equilibrium constant; and F is a ratio of cross-sections appearing in the electrical conductivity expression. It will also prove useful to define the Mach number and Alfven number by

$$M_1 \equiv u_{x_1}'/(5RT_1'/3)^{\frac{1}{2}} \; , \; M_{A_1} \equiv (\rho_1'\mu_0 u_{x_1}'^2)^{\frac{1}{2}}/B_{x_1}' \quad ,$$

which are constant for any given shock.

Consistent with the single-temperature, singly ionizing gas model postulated previously, the thermal and caloric equations are

$$p' = \rho' R(1+\alpha)T' \quad ,$$

$$\iota' = \frac{5}{2} R(1+\alpha)T' + \alpha R\Theta'_{ion} \quad ,$$

where $p'$ and $\iota'$ are pressure and specific enthalpy respectively. Using these relations and including the radiation heat flux term $\vec{q}'_r$ in the energy equation, the "inviscid" conservation and Maxwell equations associated with the normal shock geometry of Fig. 1b can be written. These, together with the dimensionless version of Eqs.(10)-(12) take the dimensionless form

$$\frac{d}{dx}(\rho u_x) = 0 \tag{15a}$$

$$\frac{d}{dx}\left\{\rho u_x\left[u_x + \left(\frac{3}{5M_1^2}\right)\frac{T(1+\alpha)}{u_x}\right] + \frac{B_z^2}{2M_{A_1}^2}\right\} = 0 \tag{15b}$$

$$\frac{d}{dx}\left\{\rho u_x u_z - \frac{B_x B_z}{M_{A_1}^2}\right\} = 0 \tag{15c}$$

$$\frac{d}{dx}\left\{\rho u_x\left[\left(\frac{3}{2M_1^2}\right)\left(T + \alpha T + \frac{2}{5}\alpha\Theta_{ion}\right) + \frac{u_x^2 + u_z^2}{2}\right.\right.$$

$$\left.\left. + \frac{3\Theta_{ion}q_r}{5M_1^2} + \frac{E_y B_z}{M_{A_1}^2}\right\} = 0, \tag{15d}$$

11

$$\frac{dB_x}{dx} = 0 \tag{15e}$$

$$\frac{dE_y}{dx} = 0 \tag{15f}$$

$$\frac{dB_z}{dx} = Rm \ (-E_y + u_x B_z - u_z B_x) \tag{15g}$$

$$\frac{d^2 q_r}{dx^2} = 3\ell_1^2 q_r + 4\pi\ell_1 \frac{dS}{dx} \tag{15h}$$

$$\frac{d\alpha}{dx} = \frac{k_{f_e}}{u_x^2} \left(\frac{\alpha}{1+\alpha}\right) \left[1 - \left(\frac{\alpha}{\alpha_{eq}}\right)^2\right] - \left(\frac{dq_r}{dx}\right) \tag{15i}$$

where $\ell_1 = \lambda_1'/\lambda_r' \simeq 6.24 \times 10^{-3}$ for argon.

Making use of Eq.(14), we can also write the functions $\alpha_{eq}$, $k_{f_e}$, Rm and S,

$$\alpha_{eq}(\alpha, T, u_x) = \left[1 + \frac{(1+\alpha)}{u_x K_{eq}(T)}\right]^{-\frac{1}{2}} \tag{16a}$$

$$k_{f_e}(T) = \frac{k_{f_e}'(T')}{(2)^{\frac{1}{2}} Q_{AA_1}' u_{x_1}'} \tag{16b}$$

$$Rm(\alpha, T) = \frac{\mu_0 e^2}{\rho_1' Q_{AA_1}'} \left(\frac{5\pi m_A^3}{48 m_e^3}\right)^{\frac{1}{2}} \frac{M_1 \alpha}{T^{\frac{1}{2}} F(\alpha, T)} \tag{16c}$$

$$S(\alpha, T, u_x) = \left(\frac{2\nu_{ion}'^3 m_A}{\rho_1' u_{x_1}' c^2}\right) \frac{T \exp(-\Theta_{ion}/T)}{\Theta_{ion}} \left(\frac{\alpha}{\alpha_{eq}}\right)^2 \left[\frac{1-\alpha_{eq}^2}{1-\alpha^2}\right] \tag{16d}$$

Equations (15a) through (15i) are nine ordinary differential equations in the nine unknowns: $\rho, u_x, u_z, T, B_x, B_z, E_y, \alpha$ and $q_r$.

The boundary conditions for this system relevant to the present problem are

at $x \to -\infty$ : $\rho = u_x = T = B_x = 1$

at $x \to -\infty$ : $u_z = B_z = \alpha = q_r = dq_r/dx = 0$ (17)

at $x \to -\infty$ : $E_y = E_{y_1}$

The integral of Eqs.(15a) through (15i) consistent with the boundary condition (17) is

$$\rho = 1/u_x \ , \ u_z = B_z/M_{A_1}^2 \ , \ B_x = 1, \ E_{y_1}$$ (18a)

$$u_x - 1 + \left(\frac{3}{5M_1^2}\right)\left[\frac{T(1+\alpha)}{u_x} - 1\right] + \frac{B_z^2}{2M_{A_1}^2} = 0$$ (18b)

$$(u_x^2-1) + \left(\frac{3}{M_1^2}\right)\left[T(1+\alpha)+ \frac{2}{5}\alpha\Theta_{ion} - 1\right] + \frac{6\Theta_{ion}q_r}{5M_1^2} + \frac{B_z}{M_{A_1}^2}\left(2E_{y_1}+ \frac{B_z}{M_{A_1}^2}\right) = 0$$ (18c)

The differential equation for the magnetic induction, Eq.(15g) becomes simply

$$\frac{dB_z}{dx} = Rm\left[-E_{y_1} + B_z\left(u_x - 1/M_{A_1}^2\right)\right]$$ (19)

The physical requirement of zero induced currents in state 1 is equivalent to requiring $(dB_z/dx) = 0$ as $x \to 0$. But since $B_{z_1} = 0$, this will happen if either $E_{y_1} = 0$ (magnetohydrodynamic shock) or $Rm_1 = 0$ (gas-ionizing

shock) or both.

Clearly if the upstream state is nonconducting $(Rm_1 = 0)$, Eq.(19) is insufficient to uniquely define $E_{y_1}$. It can however be shown that an analogy exists between chemical energy release and Joule heating within the shockfront; a fact which has led some investigators to propose a Chapman-Jouget like behavior as the criteria for determining $E_{y_1}$. Specifically, application of the Chapman-Jouget hypothesis to normal gas-ionizing shocks was suggested by Gross[2], developed further by Taussig[3,4] and has recently received some experimental confirmation in the electromagnetic shock tube work carried out by Levine[13].

Keeping the more general gas-ionizing case in mind we henceforth restrict the analysis to the special case of $E_{y_1} = 0$ (magnetohydrodynamic shock) since primary interest is focused on the qualitative influence of precursor ionization on hydromagnetic induction lengths. The generalization to $E_{y_1} \neq 0$ is straightforward however.

4. Integral Curves

It will now be shown, making the physically significantly assumption of "small" values of the parameter $\beta = \alpha$, that integral curves in $(u_x, B_z)$ phase space can be constructed for various Alfven numbers in the magnetohydrodynamic switch-on range. These curves nicely illustrate the distinction between shock structures which are fully dispersed by magnetic induction effects and those containing imbedded gasdynamic discontinuities.

Letting $E_{y_1} = 0$, the magnetic induction equation, Eq.(19) can be written in the form

14

$$\frac{dB_z}{dx} = \text{Rm}(\alpha,T)\, g(u_x,B_z) \tag{20}$$

where the function $g$ is defined by

$$g(u_x,B_z) \equiv B_z\left(u_x - 1/M_{A_1}^2\right) \tag{21}$$

Moreover, eliminating the quantity $T(1+\alpha)$ between Eqs. (18b) and (18c) gives the the quadratic equation in $u_x$:

$$f(u_x,B_z,\alpha_1,q_r) = 4u_x^2 - \left(5 + \frac{3}{M_1^2} + \epsilon_1\right)u_x + \left(1 + \frac{3}{M_1^2} - \epsilon_2\right) = 0 \tag{22}$$

where the functions $\epsilon_1$ and $\epsilon_2$ are defined

$$\epsilon_1(B_z) \equiv -\left(\frac{5}{2M_{A_1}^2}\right)B_z^2 \tag{23a}$$

$$\epsilon_2(B_z,\alpha,q_r) \equiv \left(\frac{1}{M_{A_1}^4}\right)B_z^2 + \frac{6\Theta_{ion}\alpha}{5M_1^2}\left(1 + \frac{q_r}{\alpha}\right) \tag{23b}$$

Solving $f = 0$ for $u_x$ gives the double-valued function

$$u_x(B_z,\alpha,q_r) = \frac{1}{8}\left\{5 + \frac{3}{M_1^2} + \epsilon_1 \pm \left[9\left(1 + \frac{1}{M_1^2}\right)^2 \right.\right.$$

$$\left.\left. + \epsilon_1^2 + \left(10 + \frac{6}{M_1^2}\right)\epsilon_1 + 16\epsilon_2\right]^{\frac{1}{2}}\right\} \tag{24}$$

Correspondingly, the value of $T$ is

$$T(u_x, B_z, \alpha, q_r) = \frac{1 + (M_1^2/3)\ (1 - u_x^2 - \epsilon_2)}{(1 + \alpha)} \qquad (25)$$

At this point it is instructive to examine the role of the parameter

$$\beta \equiv \frac{\alpha \Theta_{ion}}{M_1^2} \qquad (26)$$

Note first from Eq.(15i) that if one neglects electron-impact reactions $(k_{f_e} = 0)$, $d\alpha = dq_r$ so that $\alpha \geq q_r$. It follows that $q_r/\alpha$ is at most of order unity. Now suppose the parameter $\alpha$ is much less than one; in practice $\beta \ll 1$ either when $M_1$ is reasonably low (say) $M \approx 10$ and $\alpha$ is very small throughout the structure, or when $M_1$ is very large (say) $M_1 = 50$ or more and $\alpha$ becomes unity as the gas is fully ionized by the shock front. In either of these cases since $\beta \ll 1$ and $q_r/\alpha \leq 1$, it follows from Eq.(23b) that $\epsilon_2$ is virtually independent of $\alpha$ and $q_r$ and therefore that $u_x = u_x(B_z)$ from Eq.(24). It might also be pointed out that all cases of interest here correspond to $M_1^2 \gg 1$ in order to assure sufficiently high temperatures associated with ionization levels of an electrically conducting gas.

Thus, the integral curves in $(u_x, B_z)$ phase space corresponding to the limits $\beta \to 0$ and $M_1 \to 0$ can be taken as representative of a physically significant class of switch-on shocks actually generated in an apparatus of the type shown in Fig. 1a . If $Rm_1 \neq 0$, $Rm_2 \neq 0$, then the curve $g(u_x, B_z) = 0$ passes through both states 1 and 2, since $dB_z/dx = 0$ asymptotically upstream and downstream of the shock front. (The latter conditions result from requiring induced currents to vanish upstream and downstream of the shock front.) Moreover, the structure solution proceeds along the

16

$f(u_x, B_z) = 0$ curve (cf. Ref.6). The intersection of the $f = 0$ and $g = 0$ curves are the endpoints of the shock structure at states 1 and 2.

It will become evident that the monatomic gas switch-on shocks of interest here exist in the Alfven number range $1 \leq M_{A_1} \leq 2$ for the limits $\beta \to 0$, $M_1 \to \infty$. Figure 2 shows certain key integral curves associated with the structure of these shocks. The positive and negative signs before the square brackets relate to upper and lower branches of the double-valued $f = 0$ function. It can be shown that these branches are "open" when $1 \leq M_{A_1} < (8/5)^{\frac{1}{2}}$ as seen for example in Fig.(2b).

Figures (2c)-(2e) show these integral curves after the $f = 0$ function has become completely "closed" in the region $(8/5)^{\frac{1}{2}} < M_{A_1} \leq 2$. Here, a maximum value of the magnetic field on the $f = 0$ curve can be identified and computed from Eq.(24): $B_z = B_{z,max}$ when $(dB_z/du_x) = 0$. The corresponding value of $u_x$ denoted $u_{x,max}$ is given by

$$u_{x,max} = \frac{5}{8} \left\{ \frac{16}{25M_{A_1}^2} + \left[ \left(1 + \frac{16}{25M_{A_1}^2}\right)^2 - \frac{9}{25}\right] \right\}$$

At state 2, $g = 0$, so that, since $B_{z_2} \neq 0$, we get from Eq.(21)

$$u_{x,2} = \frac{1}{M_{A_1}^2}$$

Also, from Eqs.(21) and (22) we know that the sign of $B_z$ and $dB_z/dx$ is the same since $u_x > 1$ always. We can conclude therefrom that, as the structure solution proceeds along $f = 0$ from state 1 toward state 2, we

must have $B_z$ monotonically increasing or monotonically decreasing. But when $f = 0$ and $g = 0$ intersect after the "knee" of the $f = 0$ curve, as in Fig.(2e), then the only permissible path is a transition along $f = 0$ from state 1 to 1* and a subsequent "jump" at constant $B_z$ from 1* to state 2 in the value of $u_x$. The latter structure is termed a _partly dispersed shock_ while a continuous transition from state 1 to state 2 is termed a _fully dispersed shock_.

Figure 3 shows the variation of the final value of induced magnetic field $B_{z_2}$ in terms of Alfven number $M_{A_1}$. This curve is independent of any considerations of structure. Figure 4, on the other hand, illustrates the range of Alfven numbers where fully dispersed and partly dispersed shocks are found. The criteria are

$$u_{x,2} > u_{x,max}; \quad M_{A_1} < \left[ (9/5)^{\frac{1}{2}} + 1 \right]^{\frac{1}{2}} : \quad \text{fully dispersed}$$

$$u_{x,2} < u_{x,max}; \quad M_{A_1} > \left[ (9/5)^{\frac{1}{2}} + 1 \right] : \quad \text{partly dispersed}$$

## 5. Shock Structure

Having established the integral curves for our problem, we turn now to the question of the structure thickness in physical space. In particular, we seek the role of precursor ionization in structuring the shock front. Note first that the ionization effects can be decoupled from the structure profile by defining a new variable $\bar{x}$ whose differential is

$$d\bar{x} = Rmdx \tag{28}$$

Thus, in terms of $d\bar{x}_1$, Eq.(20) becomes

$$\frac{dB_z}{dx} = B_z\left[u_x - \frac{1}{M_{A_1}^2}\right] = g(B_z) \tag{29}$$

where $u_x(B_z)$ is given by Eq.(24).

Figure 5 shows the variation of the gradient $(dB_z/dx)$ in terms of local values of $B_z$ for (a) a fully dispersed shock structure and (b) a partly dispersed shock structure. Clearly, the gradient builds up from zero to some maximum value and then decreases to zero again at state 2. In the case of the partly dispersed shock $dB_z/d\bar{x}$ changes discontinuously at the point corresponding to the velocity jump discussed previously.

Equation (29) is integrable by a simple quadrature, although the origin $\bar{x} = 0$ remains to be specified. This can be done by letting $\bar{x} = 0$ at the point of maximum magnetic field gradient $g = (dB_z/d\bar{x})_{max}$. The variation of $B_z$ and $u_x$ with $\bar{x}$ for typical fully dispersed and partly dispersed shock fronts is illustrated in Fig. 6. Evidently the shock transition takes place in a distance-characterized by $\Delta\bar{x} = 0(10)$.

It remains to relate the transformed coordinate $\bar{x}$ to the physical length coordinate $x'$ if we are to assess the self-induced ionization length discussed in the Introduction. Calculation of the inverse transformation will in general require numberical integration of Eqs.(15h) and (15i).

In order to gain some insight into the transformation from $\bar{x}$ to $x$ coordinate, we will consider the special case of a partly-dispersed shock where the gas is only slightly ionized. (The slightly ionized assumption is analogous to that made in Ref. 5 by Perona and Axford).

Specifically, in addition to assuming $\beta \rightarrow 0$, we shall in addition suppose that $\alpha$ is of the order or less than $10^{-4}$ throughout the structure. This assumption allows us to neglect the effect of ionization on temperature, since $\alpha\Theta_{ion} \ll 1$ $\left[\Theta_{ion} = 610 \text{ for argon}\right]$ and the effect of Coulomb interactions on electrical conductivity. Applying these approximations, the downstream velocity, magnetic field and temperature can be expressed,

$$u_{x_2} = \frac{1}{M_{A_1}^2} \,, \quad B_{z_2} = (2/3)^{\frac{1}{2}} \left(-4+5M_{A_1}^2 -M_{A_1}^4 \right)^{\frac{1}{2}}$$

$$T_2 \simeq \frac{5M_1^2}{9} \left(1 - \frac{1}{M_{A_1}^2}\right)^2 \tag{30}$$

Similarly, the preceding approximations allow us to express the magnetic Reynolds number as

$$Rm \simeq k_1 \alpha \tag{31}$$

where $k_1 = \left(\frac{\mu_0 e^2}{\rho_1' Q_{eA}'^2}\right) \left(\frac{3\pi m_A^3}{16m_e^3}\right) \cdot \frac{M_{A_1}^2}{M_{A_1}^2 - 1}$

where we have used the fact that from Eq.(14) $F = Q_{eA}'/Q_{AA_1}'$ when the degree of ionization is small.

In making numerical estimates of $Rm$, the values of $Q_{eA}'$ given by Devoto[14] appear to be the most up-to-date and accurate ones available. Consistent with the slightly ionized assumption and a corresponding low temperature precursor, we take Devoto's value, $Q_{eA}' \approx 10^{-20}m^2 (500 < T' < 3000°K)$.

20

As an example, consider the partly dispersed shock illustrated in

Fig. 6b $M_{A_1} = (3)^{\frac{1}{2}}$ propagating in un-ionized argon at $p_1' = 1.33 \times 10^2$

$N/m^2$ ($\approx 1.00$mm Hg), $T_1' = 300°K$, $\rho_1' = p_1'(RT_1') = 2.13 \times 10^{-3}$ kg/m$^3$.

Substituting these numerical values, together with the required constants

given previously into Eq.(31) gives $Rm \approx k_1\alpha$, where $k_1 = 3.4 \times 10^{-4}$.

Knowing the relation $Rm(x) = k_1\alpha(x)$, we have from Eq.(28),

$$d\bar{x} = k_1\alpha(x)dx \qquad (32)$$

Thus, the transformation $\bar{x} \to x$ requires a knowledge of $\alpha(x)$. From

Eqs.(15h) and (15i), in the present approximation (small ionization,

precursor is ionized by photoionization since electron-atom impacts are

rare) the governing equations become,

$$\frac{d\alpha}{dx} = - \frac{dq_r}{dx} \quad ; \quad \frac{d^2 q_r}{dx^2} - 3\ell_1^2 q_r = 0 \quad ; \quad x \leq x_s$$

where $x_s$ is the location of the imbedded shock. The associated boundary

conditions are

at $x \to -\infty$ ; $\alpha = q_r = 0$

at $x = x_s$ ; $\alpha = \alpha_2$

Correspondingly, the solution is

$$\alpha(x) = \alpha_2 e^{(3)^{\frac{1}{2}}\ell_1(x-x_s)} \qquad (33a)$$

$$q_r(x) = - \alpha_2 e^{(3)^{\frac{1}{2}}\ell_1(x-x_s)} \qquad (33b)$$

Recall that $\ell_1 = \lambda_1'/\lambda_r' \simeq 6.24 \times 10^{-3}$, therefore $\ell_1 \ll 1$ \ ince the photon mean free path is much greater than the atom-atom mean free path).

Substituting Eq.(33a) into Eq.(32) and integrating such that $x = 0$ at $\bar{x} = 0$ gives

$$(3)^{\frac{1}{2}}\ell_1\bar{x} = k_1\alpha_2 e^{-(3)^{\frac{1}{2}}\ell_1 x_s}\left[e^{(3)^{\frac{1}{2}}\ell_1 x} - 1\right]$$

But since $\Delta\bar{x}$ and $\Delta x$ are at most of order 10 and $(3)^{\frac{1}{2}}\ell_1$ is of order $10^{-2}$ we can approximate $\left[e^{(3)^{\frac{1}{2}}\ell_1 x} - 1\right] \simeq (3)^{\frac{1}{2}}\ell_1 x$ and $e^{-(3)^{\frac{1}{2}}\ell_1 x_s} \simeq 1$ so that the above becomes simply $\bar{x} \simeq k_1\alpha_2 x$. But $x \equiv x'/\lambda_1'$ so we can write the physical shock thickness $\Delta L'$ as

$$\Delta L' = \frac{\Delta\bar{x}_s\lambda_1'}{k_1\alpha_2} \qquad (33)$$

For the conditions discussed previously, the upstream mean free path is $\lambda_1' \approx 5.4 \times 10^{-5}$ m. From Fig. 6a the extent of the shock in the $\bar{x}$ coordinate is $\Delta\bar{x}_s \approx 10$ while from prior calculations $k_1 \approx 3.4 \times 10^{4}$ .Substituting in Eq.(33) gives the relation $\Delta L'\alpha_2 \simeq 1.5 \times 10^{-8}$ m. Noting also from Eqs.(13) and (31) that both $k_1$ and $\lambda_1'$ are inversely proportional to density $\rho_1'$ we can conclude that the foregoing relation is density independent  Thus, if we have for example $\alpha_2 \approx 10^{-5}$, we get a shock thickness of $\Delta L' = 1.5 \times 10^{-3}$ m = 0.15 cm independent of density. This dimension is considerably less than the length of magnetic annular shock tubes commonly employed in the laboratory. Finally, it should be understood that this length is <u>independent</u> of the precursor length so long as the characteristic photoionization length is much greater than that of atom-atom collisions: $\ell_1 = \lambda_1'/\lambda_1' \ll 1$.

## 6. Concluding Remarks

Several aspects of switch-on magnetohydrodynamic shock phenomenon have been dealt with in the present study. It is found that if the analysis is restricted to a conducting upstream state (magnetohydrodynamic mode) then the switch-on shock exists in the Alfven number range $1 \leq M_{A_1} \leq 2$ for the monatomic gas model used here. Within this range, the shock front is either fully dispersed or partly dispersed with imbedded discontinuities depending on $M_{A_1}$. Moreover, the effect of precursor radiation on the overall structure dimension was studied for the case of small degrees of ionization and the Clarke-Ferrari model for photoionization. It was found that the precursor length is much greater than the magnetohydrodynamic interaction length, hence there is not appreciable influence on shock structure.

The effect of a more complex resonance radiation model for the precursor such as that proposed by Vulliet[9] can also be considered in a qualitative manner. Since the primary effect of such a phenomena would be to increase the precursor length to even greater values than those used here, the present analysis can still be considered to give a qualitatively correct picture. This is so because so long as the precursor length scale (over which ionization and electrical conductive penetrate the upstream gas) is much greater than the length scale over which magnetic induction effects take place, the overall structure will be independent of the precursor length.

23

This precursor-independence has been demonstrated herein for low ionization levels. Since the interaction lengths are expected to be even smaller for higher ionization levels, it may be anticipated that this effect extends to more highly ionized shocks as well.

## References

1.  Bleviss, Z. O., "A Study of the Structure of the Magnetohydrodynamic Switch-On Shock in Steady Plane Motion," J. of Fluid Mechanics, 9, Part 1, September 1960, pp. 49-67.

2.  Gross, R. A., "Strong Ionization Shock Waves," Review of Modern Physics, 37, 4, October 1965, pp. 724-743.

3.  Taussig, R. T., "Normal Ionizing Shock Waves with Equilibrium Chemistry in Hydrogen, " The Physics of Fluids, 8, 9, September 1965, pp. 1616-1627.

4.  Taussig, R. T., "Normal Ionizing Shock Waves with Equilibrium Chemistry in Hydrogen, The Physics of Fluids, 9, 3, March 1966, pp.421-430.

5.  Perona, G. E. and Axford, W. I., "Structure of a Normal Ionizing Shock Wave in Argon," The Physics of Fluids, 11, 2, February 1968, pp.294-302.

6.  Hoffert, M. I., "Nonequilibrium Structure of Hydromagnetic Gas-Ionizing Shock Fronts in Argon," The Physics of Fluids, 11, 1, January 1968, pp.77-88.

7.  Hoffert, M. I and Lien, H., "Quasi-One-Dimensional Gas Dynamics of Partially Ionized Two-Temperature Argon," The Physics of Fluids, 10, 8, August 1967, pp. 1769-1777.

8. Clarke, J. H. and Ferrari, G., "Gas Dynamics with Nonequilibrium Radiative and Collisional Ionization," The Physics of Fluids, 8, 12, December 1965, pp.2121-2139.

9. Vulliet, W. G., "Effect of Resonance Radiation on the Transfer of Shock Precursor Radiation," The Physics of Fluids, 11, 6, June 1968, pp. 1377-1379.

10. Zel'dovich, Ya.B. and Raizer, Yu. P., Physics of Shock Waves and High Temperature Hydrodynamic Phenomena, 1, Academic Press, New York, 1966, pp. 386-406.

11. Rustgi, O. P., "Absorption Cross Sections of Argon and Methane between 600 and 170 Å," J. of the Optical Society of America, 54, 4, April 1964, pp.464-466.

12. Vincenti, W. G. and Kruger, C. H., Introduction to Physical Gas Dynamics, New York, 1965, p. 497.

13. Levine, L. S., "Experimental Investigations of Normal Ionizing Shock Waves," The Physics of Fluids, 11, 7, July 1968, pp. 1479-1486.

14. Devoto, R. S., "Transport Coefficients of Partially Ionized Argon," The Physics of Fluids, 10, 2, February 1967, pp. 354-364.

AXIAL FIELD CIRCUIT

DRIVE CURRENT CIRCUIT

EXTERNAL AXIAL FIELD SOLENOID

INTERNAL AXIAL FIELD SOLENOID

SHOCK FRONT

$U'_{x_1}$

$Y'$

$X'$

$Z'$ ⊙

① ②

(a)

$E'_{y_1}, J'_{y_1} = 0$

$U'_{x_1}, B'_{x_1}$

$U'_{z_1} = 0$

$B'_{z_1} = 0$

$\sigma'_1 \neq 0$

①

$x'$

$y'$

$z'$

$E'_{y_2}, J'_{y_2} = 0$

$U'_{x_2}, B'_{x_2} = B'_{x_1}$

$U'_{z_2}, B'_{z_2}$

$\sigma'_2 \neq 0$

②

(b)
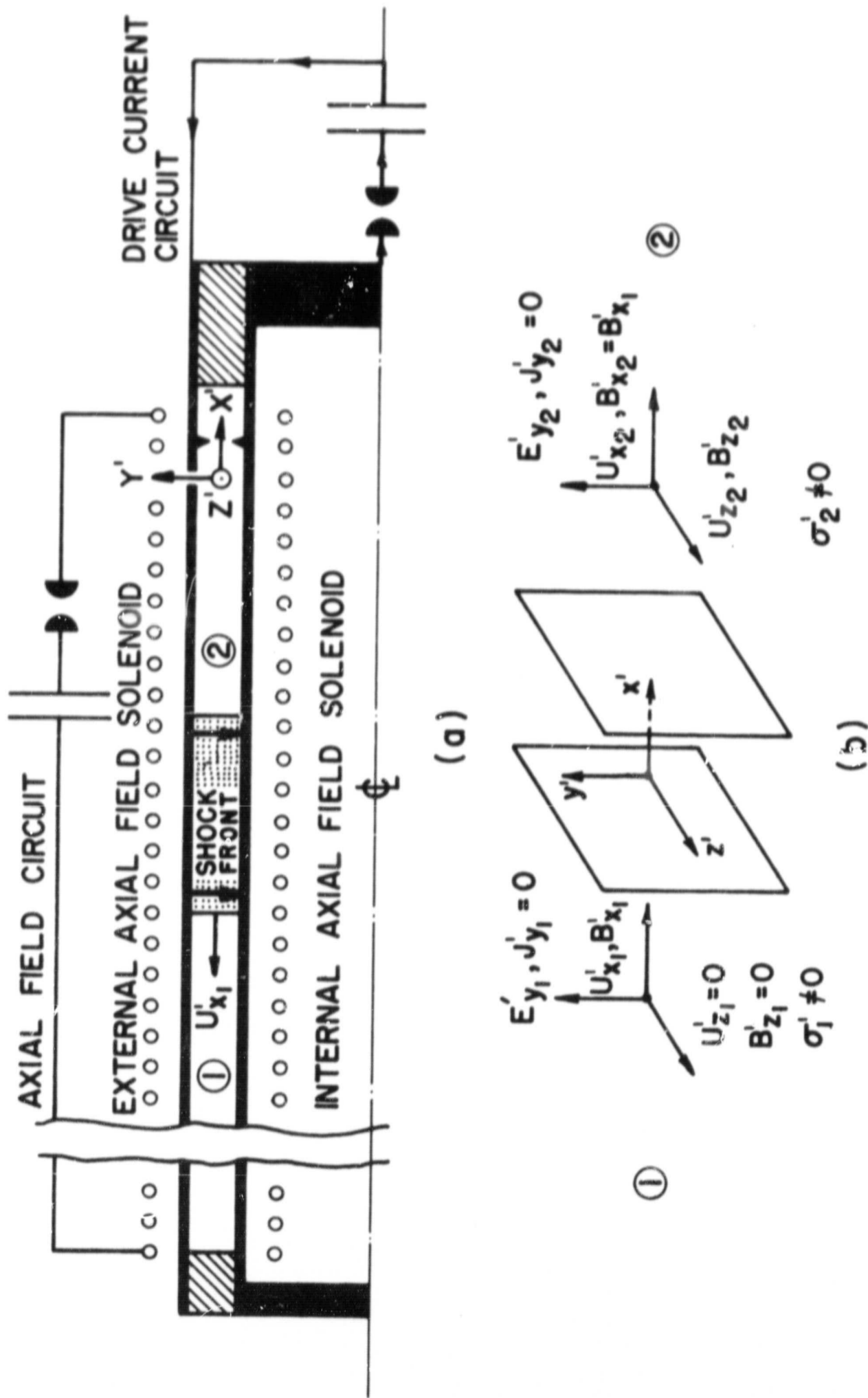
Fig. 1 (a) Schematic diagram of magnetic annular shock tube.

(b) Switch-on MHD shockfront geometry in shock-fixed coordinate system moving with velocity $-u_{x_1}$ into undisturbed gas.
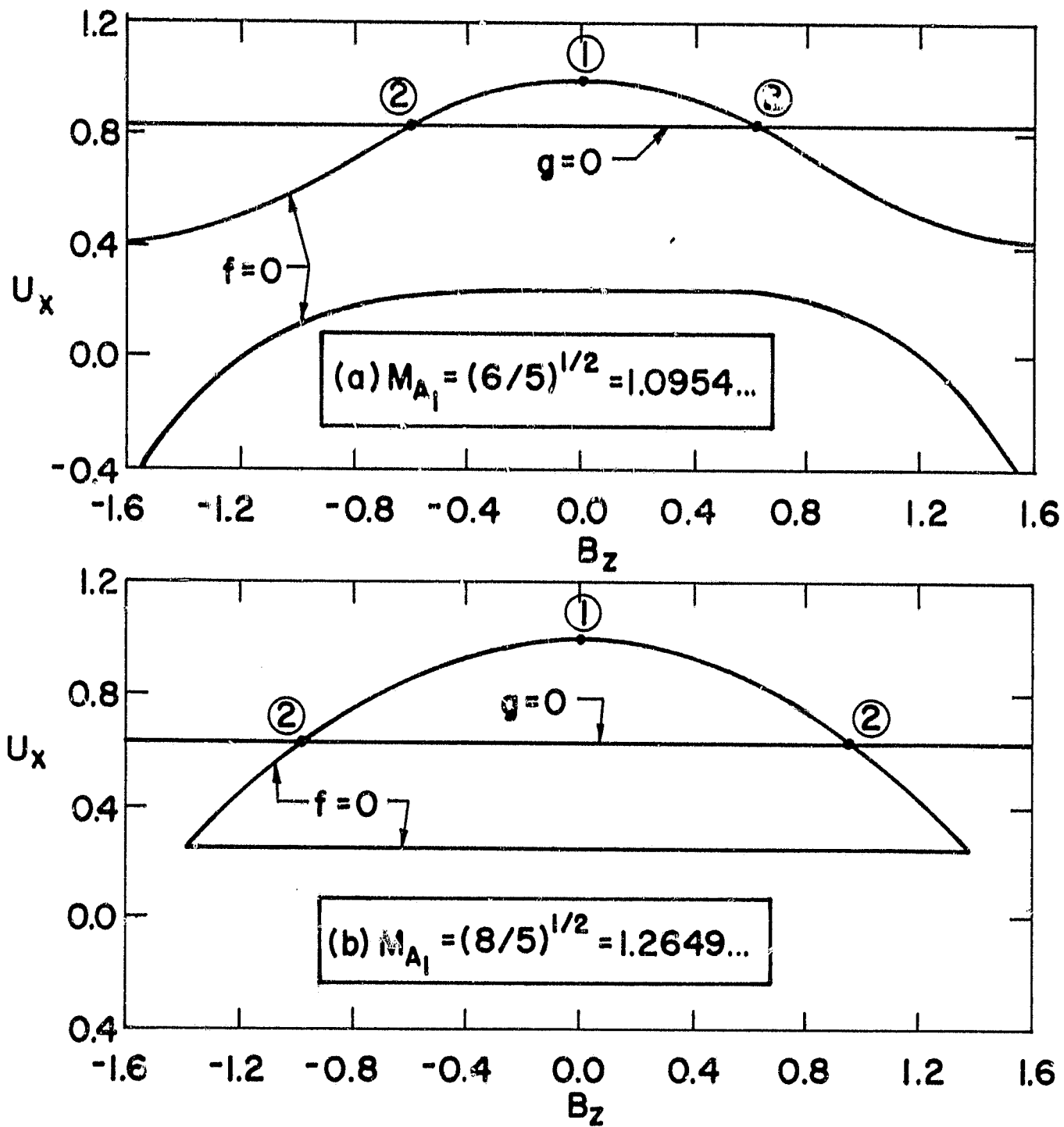
Fig. 2  Integral curves in $(u_x, B_z)$ space with $(\alpha\Theta_{ion}/M_1^2) \to 0$
for various Alfvén numbers between $M_{A_1} = 1.0$ and $M_{A_1} = 2.0$.

The solution for a negligible viscosity switch-on shock
structure proceeds alnng the $f = 0$ curved from state 1 to
state 2.  Transitions from state 1 to $1^*$ are imbedded
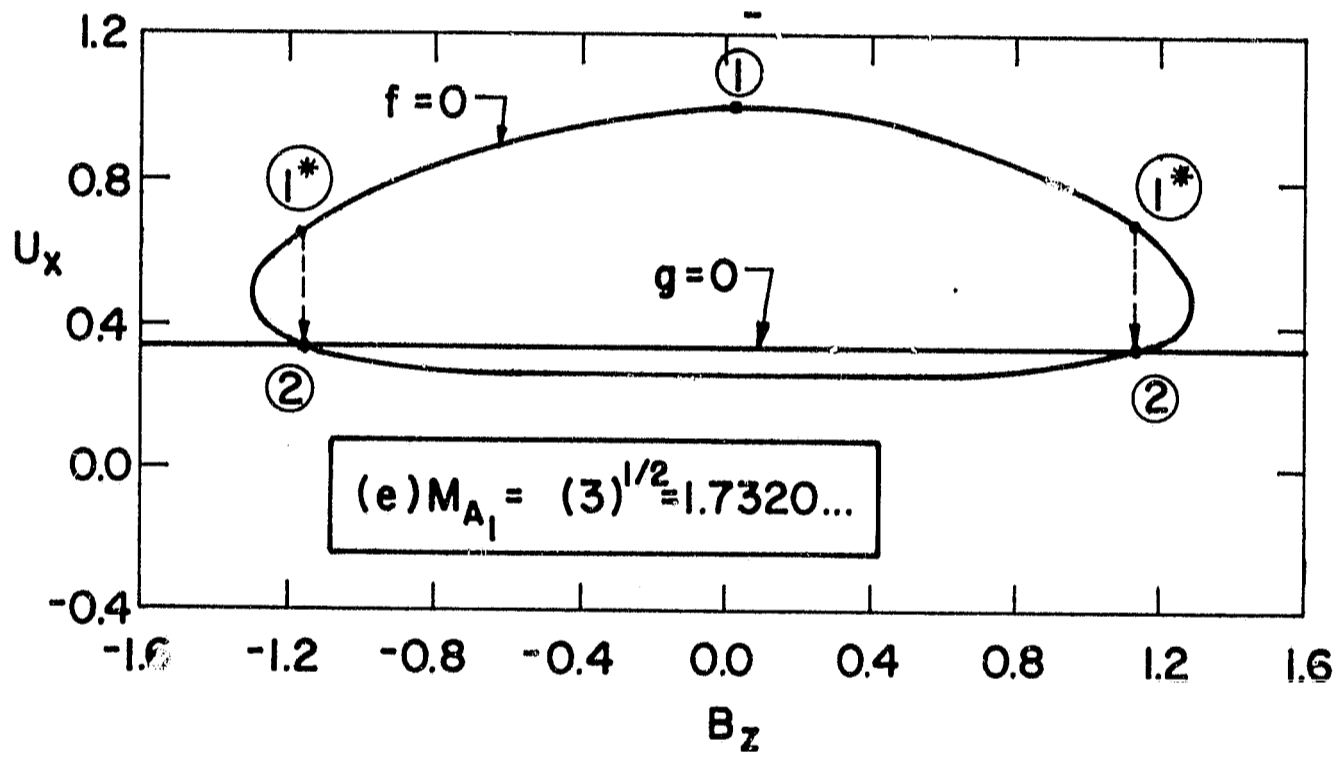(viscosity-structured) "discontinuities"

(c) $M_{A_1} = (2)^{1/2} = 1.4142...$

$U_{x_{max}} = U_{x_2}$
$B_{z_{max}} = B_{z_2}$

(d) $M_{A_1} = \left[ (9/5)^{1/2} + 1 \right]^{1/2} = 1.5302...$
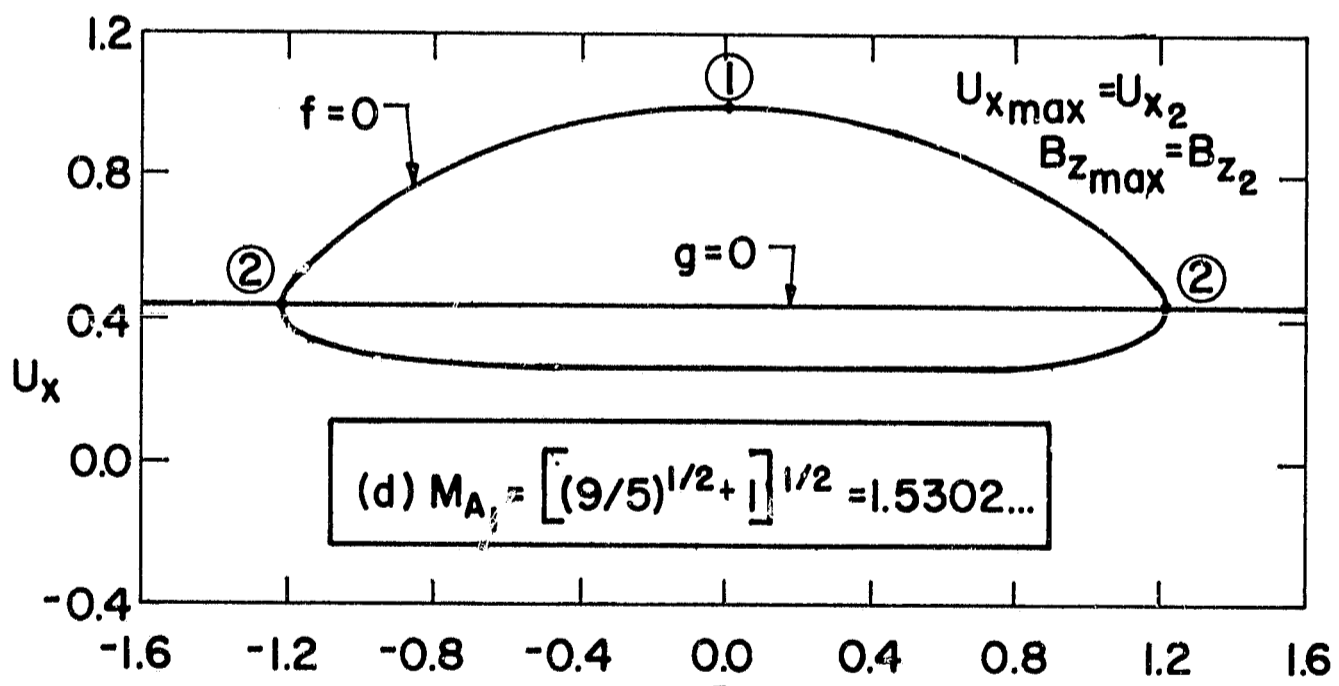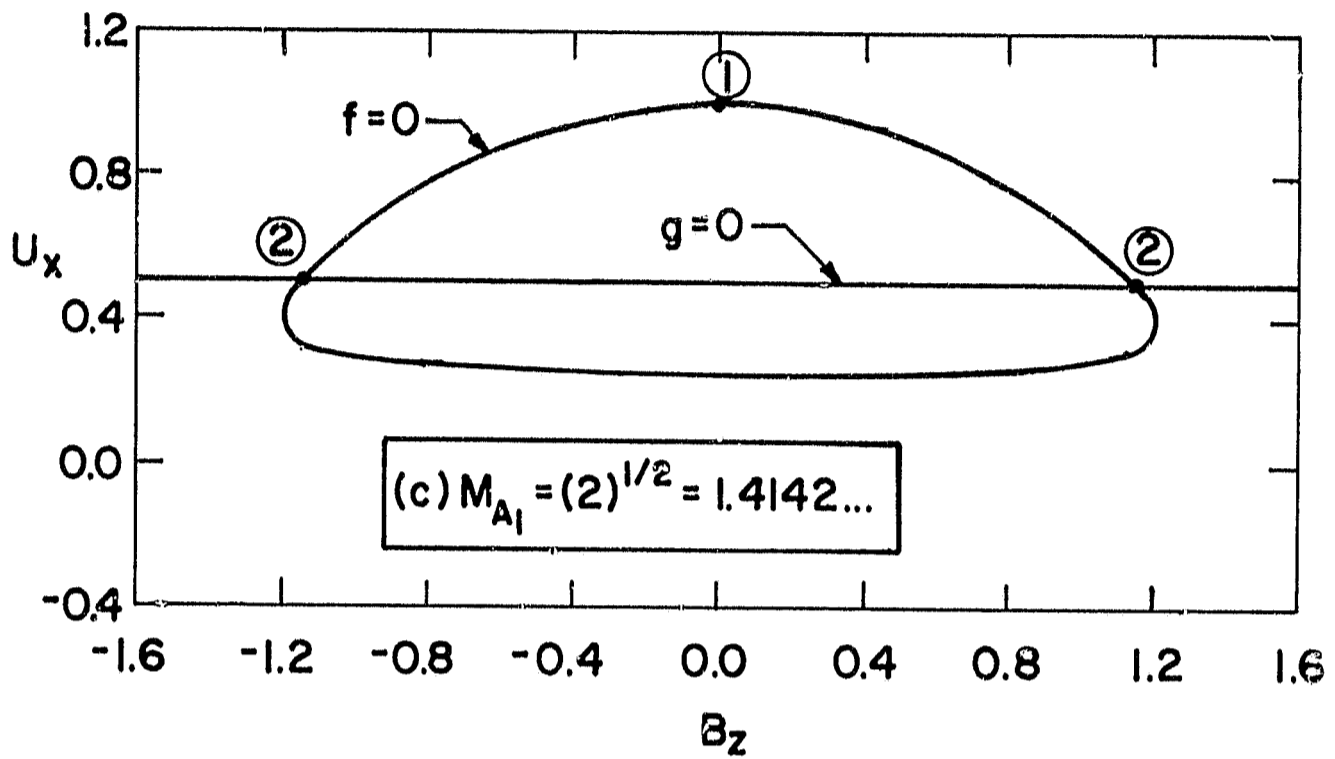
Fig. 2    Cont'd

Fig. 2   Cont'd
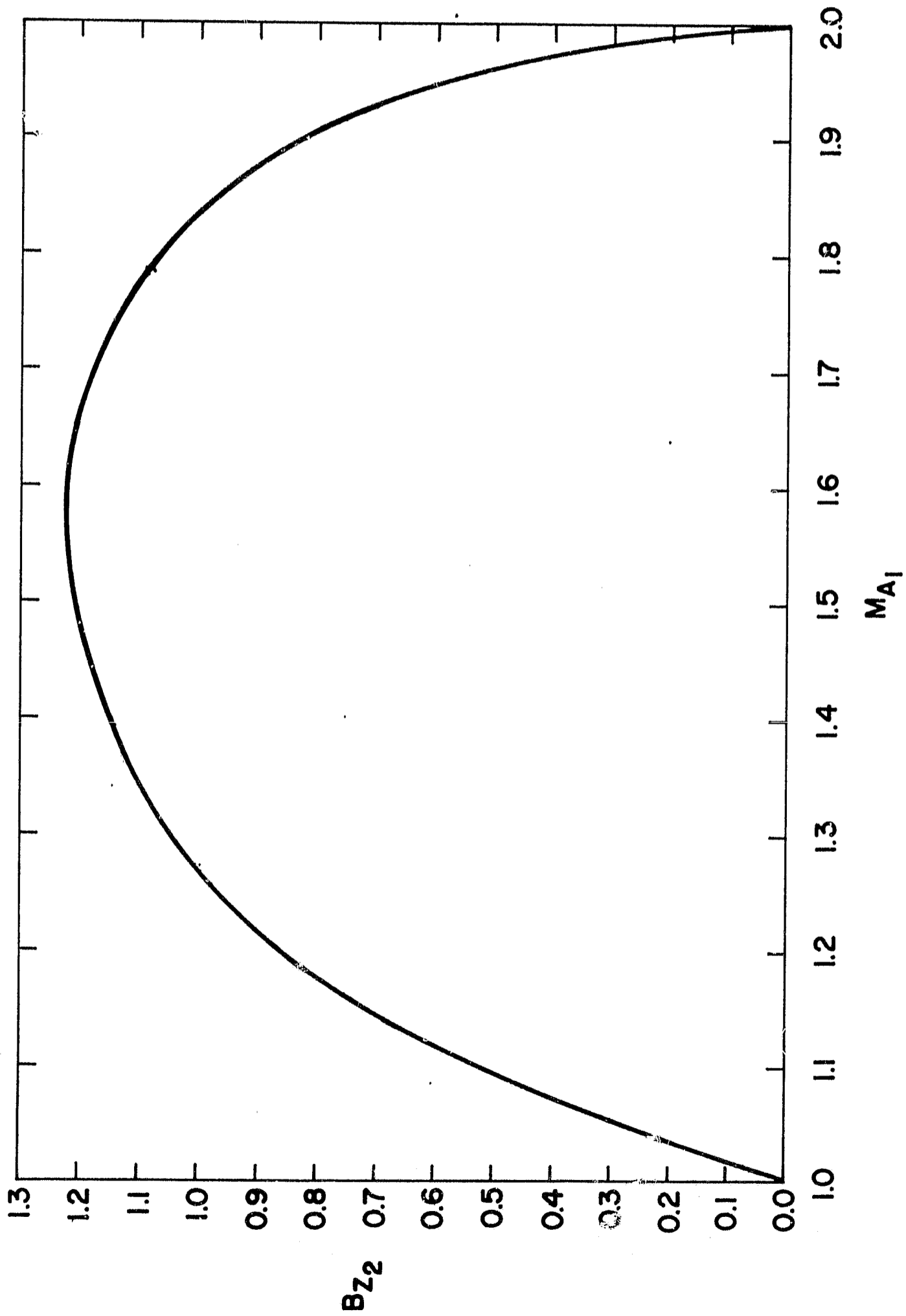
Fig. 3  Variation of final value of induced magnetic field $B_{z_2} = (B'_{z_2}/B'_{x_1})$ with shock Alfvén number when $(\alpha \otimes_{ion}/M_1^2) \to 0$.
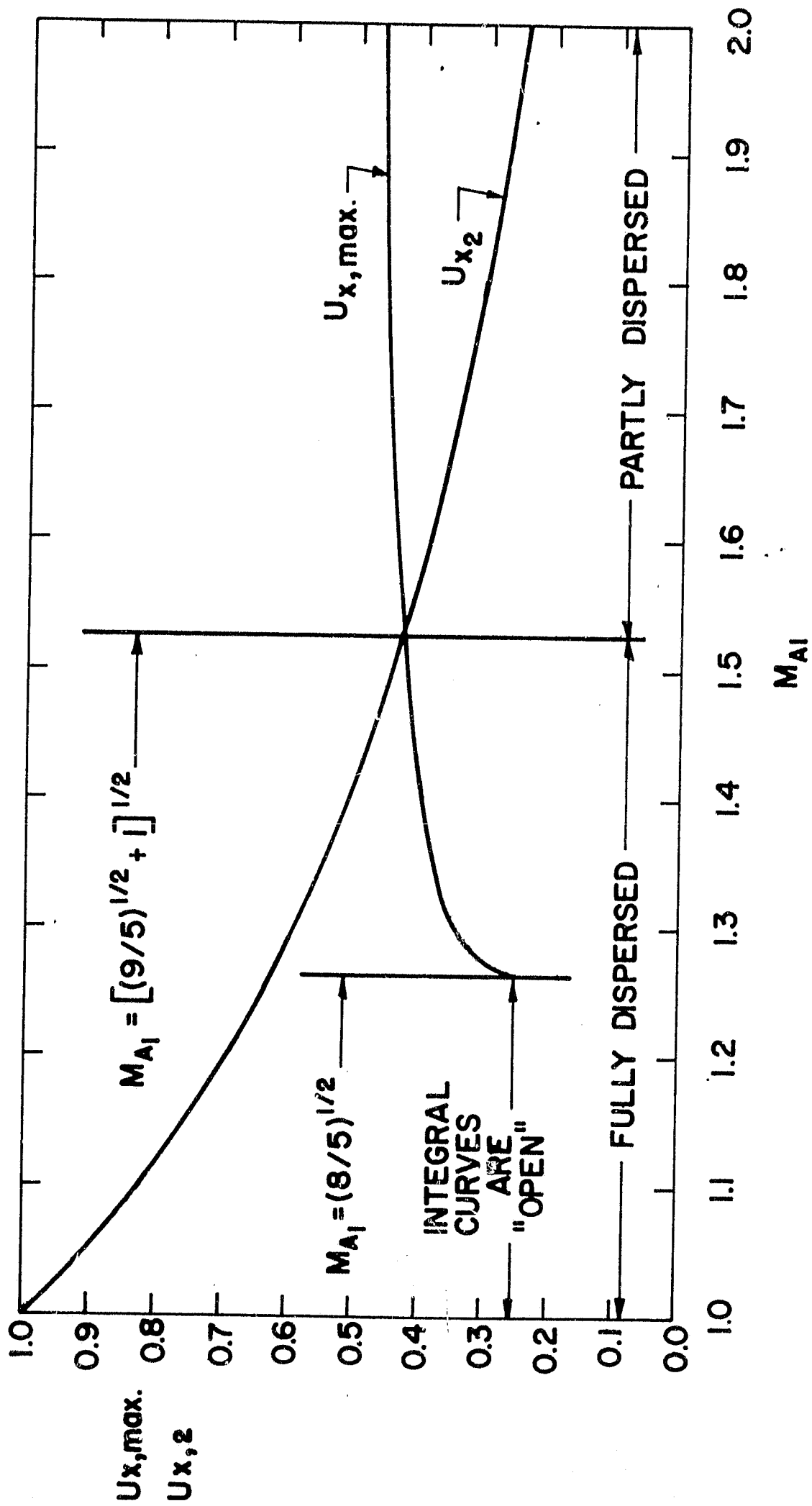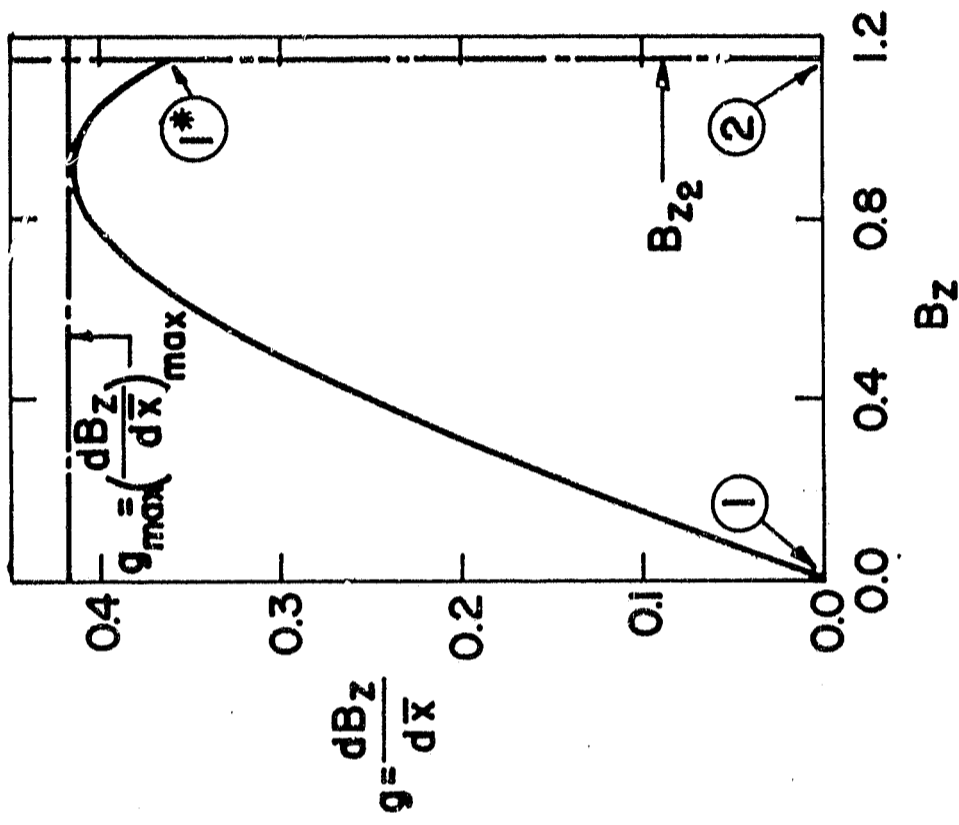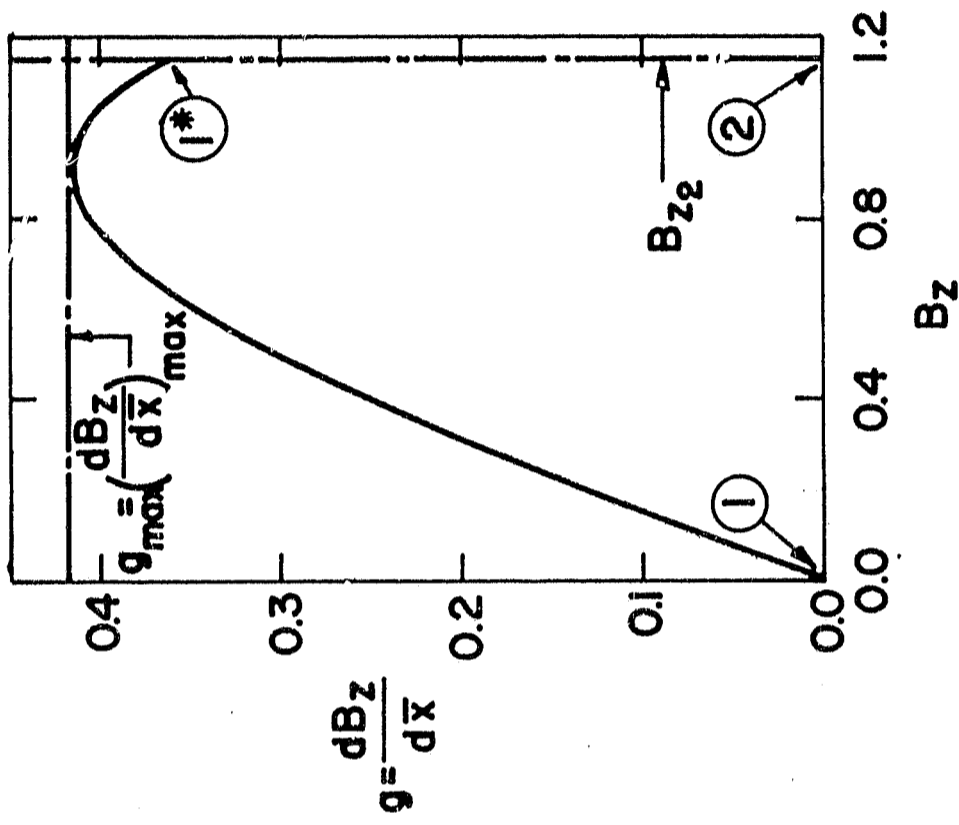
Fig. 4  Variation of maximum and final velocity with Alfvén number when $(\alpha\Theta_{ion}/M_1^2) \to 0$.  The crossover point distinguishes between fully dispersed and partly dispersed regimes.

Fig. 5 Variation of magnetic field gradient versus induced field. The point where $g = (dB_z/d\bar{x})_{max}$ was chosen as $\bar{x} = 0$ in the structure calculations.

(a) FULLY DISPERSED STRUCTURE, $M_{A_1} = (2)^{1/2}$

(b) PARTLY DISPERSED STRUCTURE, $M_{A_1} = (3)^{1/2}$

(a) FULLY DISPERSED STRUCTURE, $M_{A_1} = (2)^{1/2}$
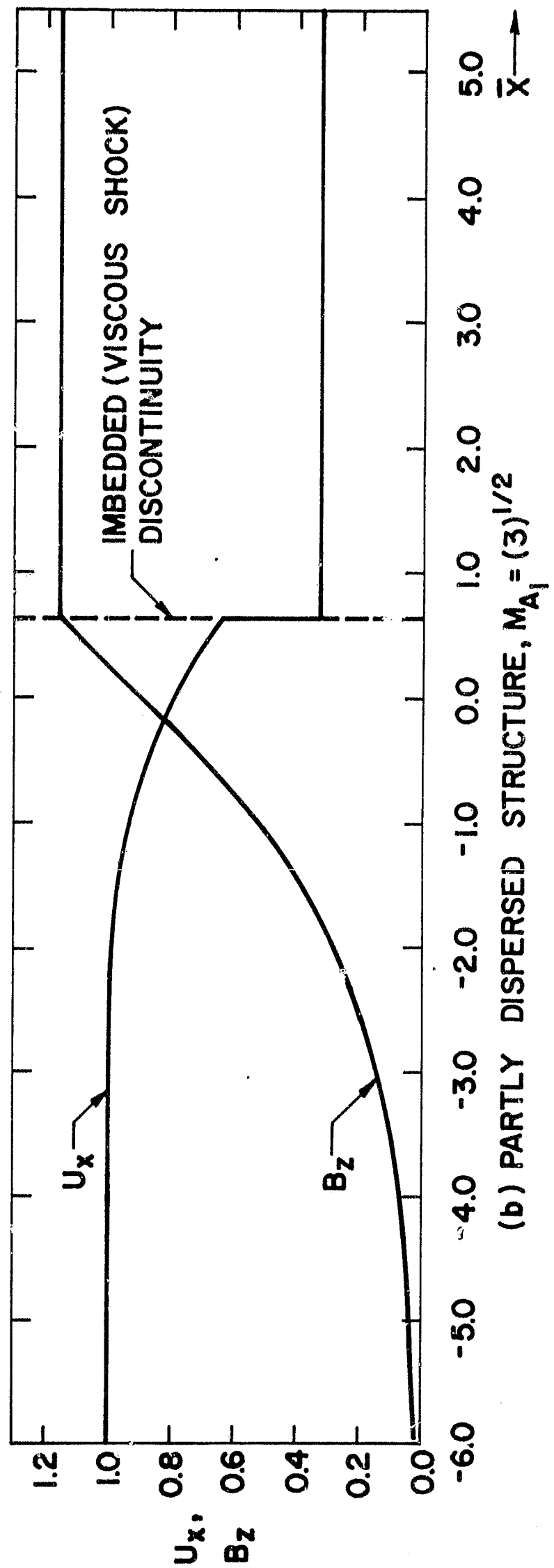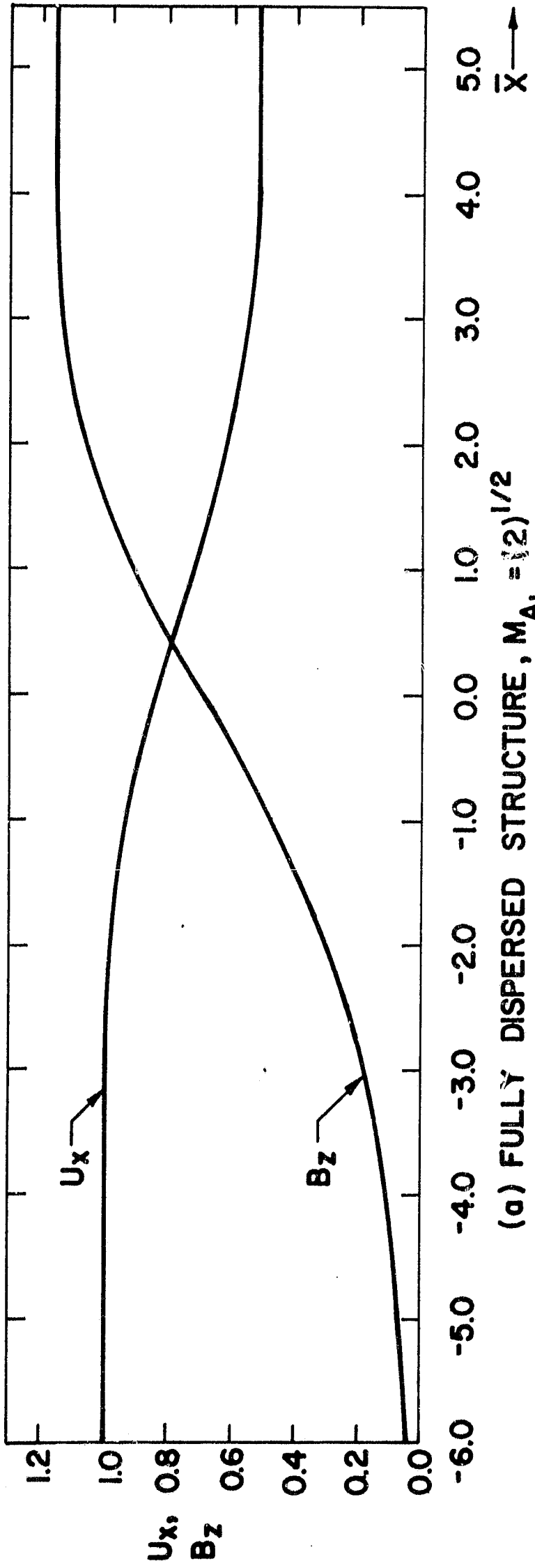
(b) PARTLY DISPERSED STRUCTURE, $M_{A_1} = (3)^{1/2}$

Fig. 6 Shock structure in terms of the "stretched" variable $\bar{x}$ ($d\bar{x} = Rmdx$)

31